Properties and Device Applications of Magnetic Domains in Orthoferrites

By A. H. BOBECK

(Manuscript received August 15, 1967)

It has been shown that isolated magnetic domains in thin platelets ($\approx$2 mils thick) of orthoferrites can be manipulated to perform memory, logic, and transmission functions. The purpose of this paper is to discuss the properties of orthoferrites that make them suitable for magnetic device applications and consider magnetostatic problems relevant to domain structures found to be useful. Included is a brief indication of how memory, logic, and transmission can be accomplished; however, the details will be reserved for a later paper.

The stability conditions of a cylindrical domain are discussed in detail and data is reported to support the conclusions. Of particular interest are the sizes of cylindrical domains available in the various orthoferrites. Such data has been taken on five of the fourteen possible orthoferrites and it is found that the thulium orthoferrite, $TmFeO_3$, gives the smallest stable domain diameter (2.3 mils) and $LuFeO_3$ the largest. The stability results lead to a direct method for obtaining σ_W, the domain wall energy density. For $TmFeO_3$, as an example, $\sigma_W = 2.8$ ergs/cm^2.

It is concluded that the orthoferrites are well suited indeed for device applications. Experimentally, 3 mil diameter domains have been manipulated and there is every reason to believe that operation of sub-mil domains will soon be realized.

I. INTRODUCTION

Recently, P. C. Michaelis described a technique for propagating isolated magnetic domains in thin anisotropic ferromagnetic films.[1] He obtained controlled motion along either the easy (e) or hard (h) anisotropy axis although he used distinctly different mechanisms to obtain propagation in these directions.

Michaelis' ferromagnetic films were processed to have a uniaxial anistropy (i.e., hard and easy axis) in the plane of the film. Magneti-

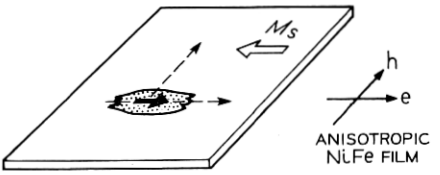

Fig. 1 — An isolated magnetic domain can be moved along the easy (e) or the hard (h) anisotropy axis.

zation lies in the plane of the film and a magnetic domain, as illustrated in Fig. 1, is seen to be an isolated reverse magnetization area bounded by a domain wall. The disparity in the propagation modes for the e and h directions is due to anisotropy inherent in the film itself. Propagation of domains along the diagonals is possible using conventional wall propagation and, in fact, Spain[2] has recently discussed such a technique.

Complete generality in the propagation (and interactions) of magnetic domains, however, demands that the magnetization be aligned *normal* to the surface of the film. Furthermore, it would be useful if the magnetic properties were isotropic (or essentially so) in the plane of the film. A cylindrical domain in such a material is drawn in Fig. 2. These conditions are met in orthoferrites as first pointed out by R. C. Sherwood. Other similar materials are magnetoplumbite, barium ferrite, and manganese bismuth.

This memorandum will describe some of the results of generating and propagating cylindrical domains. Related magnetostatic problems are introduced and discussed. It will be shown that the stability conditions for cylindrical domains lead to a method of determining wall energies and results obtained so far on orthoferrites are tabulated. Finally, a brief description is given of some of the

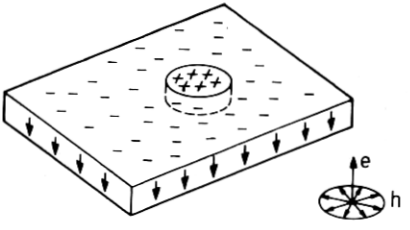

Fig. 2 — An ideal material permits magnetization normal to platelet surface and is otherwise isotropic.

device properties; however, this aspect will be treated in much more detail in a later memorandum.

II. ORTHOFERRITES

An excellent treatment of orthoferrites can be found in Ref. 3. Orthoferrites of the general formula $MFeO_3$, where M is any rare earth ion are antiferromagnetic with a weak ferromagnetism caused by a slight canting (0.5°) of the antiparallel spins. The molecular and magnetic unit cell is an orthorhombic cell of sides a, b, and c with the c side about twice the length of a or b, as illustrated in Fig. 3. The antiparallel Fe 3+ spins align along the a-axis with the c-axis exhibiting the weak ferromagnetism ($4\pi M_s \approx 100$ gauss). The lone exception is $SmFeO_3$ which has its net moment along the a-axis at room temperature. The Néel temperature for all orthoferrites is about 400°C.

The orthoferrites have a remarkable set of magnetic properties. When magnetized to saturation, fields of several thousand oersteds are needed to effect a flux reversal. This field (nucleation field H_N) is an order of magnitude greater than the magnetic moment of a typical orthoferrite. Thus, platelets having the c-axis normal to the planar surface are magnetically stable without an applied field even when fully saturated. Furthermore, once domain walls are present they can be moved with fields (wall coercivity H_c) less than one oersted. Thus,

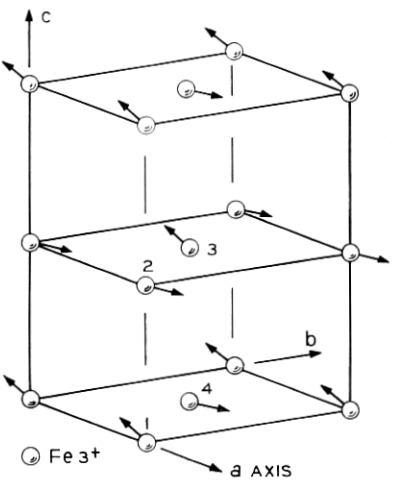

Fig. 3 — Locaton of Fe^{3+} spins in typical orthoferrite orthorhombic cell.

the orthoferrites are ideally suited for device applications which utilize materials with a reentrant *B-H* hysteresis characteristic.

Orthoferrites can be grown from a PbO flux and all of the specimens evaluated during the course of this work were so prepared by J. P. Remeika and L. J. VanUitert. Occasionally, a particular run will yield nearly perfect single crystal platelets of orthoferrite. Dimensions vary with 0.1 inch by 0.2 inch by 2 mils thick being typical. Fortunately, most of these platelets grow with the *c*-axis normal to the plane and are thus ideally suited for cylindrical domain observations.

The tendency to grow platelets is not characteristic of all orthoferrites. For this reason, it has been necessary to develop techniques for preparing platelets from larger crystals.

Orthoferrites are optically transparent, especially to the red spectrum. Magnetic domains in a thin platelet (2.3 mils thick) of $TmFeO_3$ are readily seen using the Faraday rotation of transmitted light. Note in Fig. 4 the random orderliness of the areas magnetized up (dark) and down (light). Magnetostatic and wall energies balance to determine the general shape as well as the dimensions of the domains. It is only with a great deal of reluctance that these domains yield to an inhomogeneous field.

III. MAGNETOSTATICS AND STABILITIES OF STRIPS AND CYLINDERS

Assume, as pictured in Fig. 5, that a loop of wire is placed in contact with the surface of an orthoferrite platelet. When a current

X 16

Fig. 4 — Faraday observation of magnetic domains in $TmFeO_3$. Note the isolated oval domain.

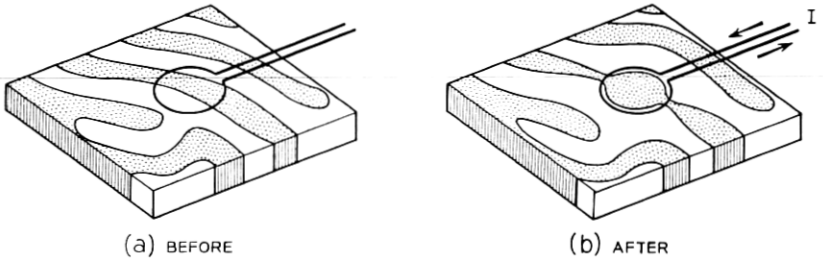

Fig. 5 — In the process of generating a cylindrical domain a current applied to a loop alters the static domain pattern of (a) to that of (b).

is applied to the loop the resulting field pattern will perturb the existing domains. Areas of magnetization seeing a favoring applied field will grow — others will shrink. To produce a cylindrical domain, note that it will be necessary to "pinch off" at several points. To maintain a cylindrical domain when the applied current, I, is removed, it is usually necessary to apply a dc bias field normal to the surface of the platelet. The conditions under which the cylindrical domain is stable will be analyzed in this section.

3.1 *Magnetic Strip Domain*

To a first approximation, the field necessary to "pinch" a strip domain to produce a cylindrical domain can be equated to the field required to compress a strip domain to zero width. The strip resists compression since a high magnetostatic energy state is generated. The magnetostatic field effective when the strip approaches zero width can be obtained by inspection and is $4\pi M_s$ (see Fig. 6). One immediately sees the significance of the low moment of the orthoferrites since the applied fields necessary to generate cylindrical domains will be directly related to the magnetic moment.

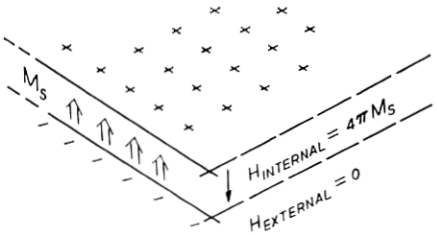

Fig. 6 — The internal magnetostatic field in a uniformly magnetized platelet is $4\pi M_s$.

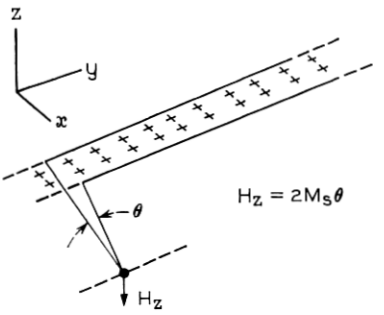

Fig. 7 — Normal magnetostatic field component generated by a strip of magnetic charge is related to the angle θ.

The relationship between the width W of a strip domain and the applied field H_s will now be discussed. (Refer to Fig. 7.) Consider a strip of magnetic charge located in the xy plane and extending to infinity in the $+y$ and $-y$ directions. The magnetic field component perpendicular to the xy plane, H_z, is directly related to the angle θ subtended by the strip and is given by $H_z = 2M_s\theta$. (A similar relationship exists for a strip carrying a uniform current.)

Consider a strip domain of width W in an orthoferrite platelet of thickness h. This case is illustrated in Fig. 8. By means of the angle relationship discussed above the z-component of field, produced by the magnetic surface charges, can be quickly obtained. For example, the field at the midpoint of either domain wall (sides of the strip) is

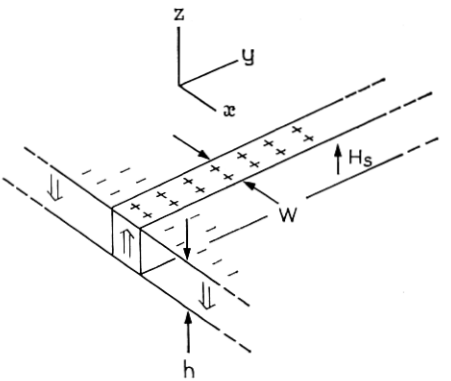

Fig. 8 — The applied field necessary to sustain a strip domain is derived in the text.

$$H(z = h/2) = 8M_s \tan^{-1} h/2W. \quad (1)$$

The polarity of this field is such as to cause the strip to widen. An applied field, equal in magnitude and opposite in sign, is, therefore, needed to maintain the strip at a width W.

More significant is the *average* field effective on the walls under the assumption that the walls are rigid (do not bulge outward). In Appendix A the desired relationship is derived and is

$$\frac{H_s}{4\pi M_s} = \frac{2}{\pi}\left[\tan^{-1}\left(\frac{h}{W}\right) - \frac{W}{2h}\ln\left(1 + \frac{h^2}{W^2}\right)\right]. \quad (2)$$

A similar expression is found in Kooy and Enz.[4] Equation (2) is plotted in Fig. 9. Note that as the strip narrows ($W \to 0$) the normalized field approaches unity as discussed previously. For a very wide strip the field effective on the wall tends to zero and the walls are stable in position without an external applied field.

Equation (2) tells us to what extent the surface charge of the strip and the sheet cancel. As W increases, the walls see cancelling fields from the surrounding magnetic charge and the wall field reduces to a low value. If the strip is driven closed, however, the quantity of nullifying charge on the strip itself goes to zero and the full internal field $4\pi M_s$ is felt. If the wall coercivity, H_c, is very low only very wide strips ($W \gg h$) will be stable in the absence of an applied field.

3.2 *Cylindrical Magnetic Domains*

In the derivation of equations which related to the performance of a strip domain, it was not necessary to include a domain wall energy

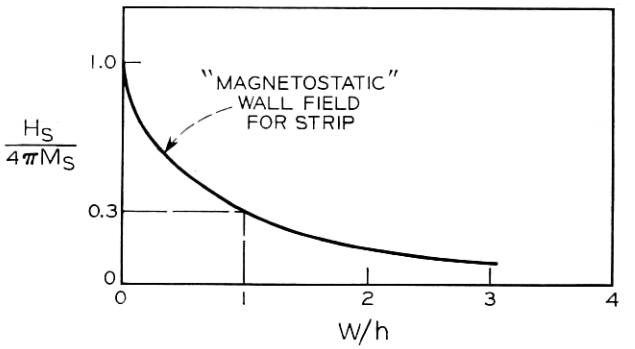

Fig. 9 — An applied field of $4\pi M_s$ is necessary to collapse a strip to zero width.

term since the walls maintained constant area. Such is not the case for a cylindrical domain.

Consider as shown in Fig. 10 a cylindrical domain of radius r in a platelet of orthoferrite of thickness h. Assume that the domain wall which defines the cylindrical domain has straight sides, i.e., the shape is neither "hour-glass" nor "barrel" like. The total energy, relative to a uniformly downward magnetized platelet can be written as

$$\xi_T(\text{total}) = \xi_W(\text{wall}) + \xi_D(\text{magnetostatic}) + \xi_H(\text{applied})$$

or,

$$\xi_T = 2\pi rh\sigma_W - \xi_D + 2M_s H_A \pi r^2 h,$$

using CGS units where the domain wall energy density σ_W is in ergs/cm^2. The partial derivative of the energy with respect to r gives the force on the wall.

$$\frac{\partial \xi_T}{\partial r} = 2\pi h\sigma_W - \frac{\partial \xi_D}{\partial r} + 4\pi rhM_s H_A \ .$$

It is assumed that $\partial\sigma_W/\partial r$ is negligible. In terms of fields,

$$\frac{\partial \xi_T/\partial r}{4\pi M_s rh} = \frac{\sigma_W}{2rM_s} - \frac{\partial \xi_D/\partial r}{4\pi M_s rh} + H_A \ . \tag{3}$$

$$(I) \qquad (II) \qquad (III) \quad (IV)$$

Equation (3) is a stability relationship in terms of magnetic fields. It relates the net effective field on the wall (*I*) to the wall field (*II*) trying to compress the cylindrical domain, the demagnetization field (*III*) trying to expand that domain, and the applied field (*IV*). If the net field (*I*) is positive the domain will compress, if it is negative it will expand.

It is convenient to express the "wall energy" and "magnetostatic" contributions as fields. Term (*II*) can be equated to a wall field,

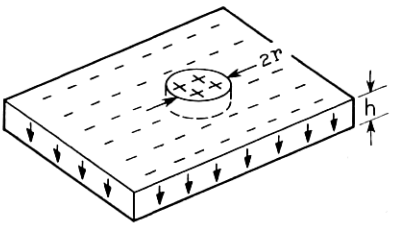

Fig. 10 — A cylindrical domain in a platelet of thickness h.

termed H_W, since it is the field contributed by the wall energy density, σ_W. So

$$H_W = \frac{\sigma_W}{2rM_s}. \tag{4}$$

Note that this field, which goes as $1/r$, is the eventual cause of the collapse inward of the smallest domains. The importance of (4) which is plotted in Fig. 11 cannot be overstressed since it points out the significant role that wall energy will play in orthoferrite devices.

A. Thiele[5] has obtained an expression in closed form for (*III*) the magnetostatic field which we shall designate as H_D. A derivation of the magnetostatic energy ξ_D is not readily obtainable. An alternative derivation, somewhat simpler but less rigorous than the technique employed by Thiele, is presented in Appendix B. The result (by either method) is

$$\frac{H_D}{4\pi M_s} = \frac{2}{\pi}\left[-\frac{2r_0}{h} + \sqrt{1 + (4r_0^2/h^2)}E(k, \pi/2)\right], \tag{5}$$

where $E(k, \pi/2)$ is the complete elliptic integral of the second kind and

$$k^2 = \frac{1}{1 + (h^2/4r_0^2)}.$$

The normalized magnetostatic field plots much (see Fig. 12) as the strip field of Section 3.1. The sense of H_D is always to attempt to expand the cylindrical domain. Equation (5) is plotted in detail in Fig. 24.

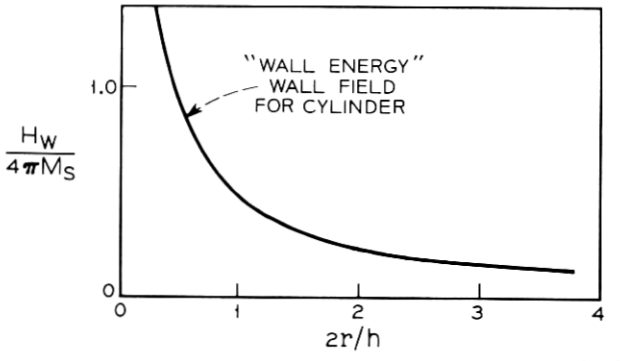

Fig. 11 — The wall energy, σ_W, generates a field of a sense to collapse a cylindrical domain.

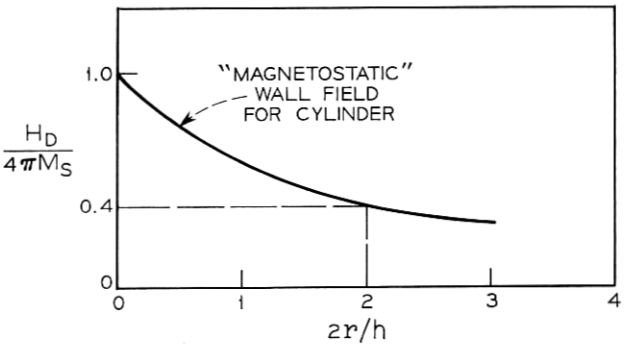

Fig. 12 — The magnetostatic energy generates a field which attempts to expand a cylindrical domain.

It is probably well to reiterate that the fields H_A, H_W, and H_D are assumed to be acting on a rigid cylindrical domain wall and H_W and H_D have no significance unless applied to the domain wall itself.

3.3 *The Stability of a Circular Domain*

We are now in a position to discuss the stability of a cylindrical domain. Three cases will be considered. They are (*i*) $r \ll h$, a very thick platelet, (*ii*) $r \gg h$, a very thin platelet, and (*iii*) $r \approx h$, a "just right" platelet. Case (*i*) will be magnetostatic energy dominated, case (*ii*) wall energy dominated, and case (*iii*) will have these energies somewhat in balance.

3.3.1 *Very Thick Platelet*

For a cylindrical domain of radius r in a platelet of thickness h, where $r \ll h$, the magnetostatic field H_D of (5) may be approximated as $4\pi M_s$. In this case the critical radius, r_a, is obtained by equating the magnetostatic field to the wall field. This is graphically done in Fig. 13. Analytically,

$$4\pi M_s = \frac{\sigma_W}{2r_a M_s}$$

and

$$r_a = \frac{\sigma_W}{8\pi M_s^2}. \tag{6}$$

For typical orthoferrites, r_a is the order of 0.5 mil. Domains of a radius greater than r_a will expand uncontrollably while those of radius

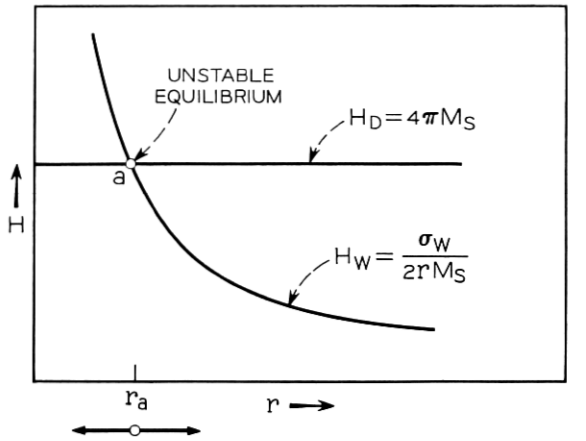

Fig. 13 — Metastable equilibrium exists with "very thick" platelets.

less than r_a will contract to oblivion. The significance of r_a is that it gives an absolute lower bound on the stable domain size. Note that the problem of initially establishing a domain of radius r_a has been carefully avoided.

3.3.2 *Very Thin Platelet*

At the other extreme are the conditions that exist in a very thin platelet, i.e., $r \gg h$ and the wall field completely dominating the magnetostatic field. Note Fig. 14. In the absence of a coercivity the criti-

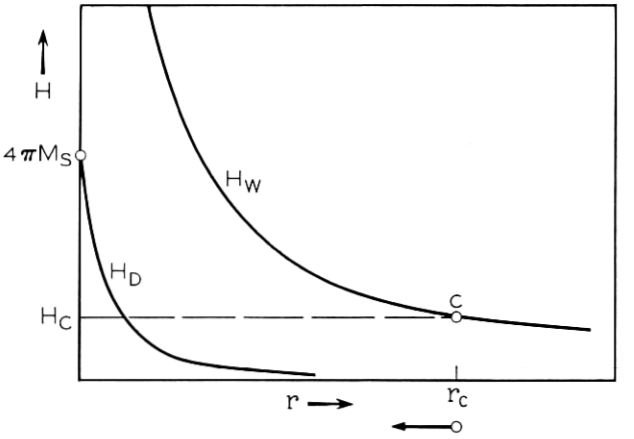

Fig. 14 — Stability condition for a "very thin" platelet.

cal radius r_c will approach infinity. With a wall coercivity H_c the minimum stable radius can be obtained from

$$H_c = \frac{\sigma_W}{2r_c M_s}$$

or

$$r_c = \frac{\sigma_W}{2M_s H_c}. \tag{7}$$

For typical orthoferrites, r_c is 40 mils. Indeed, difficulty is experienced in generating domain patterns of any kind in very thin (less than one mil) platelets.

3.3.3 *"Just Right" Platelets*

We have seen that cylindrical domains in very thick platelets are completely unstable. Also, that in very thin platelets only excessively large domains are stable and then only if some form of wall pinning is assumed.

A stable cylindrical domain can be obtained if the thickness h of the platelet is chosen so that at the point of intersection of the H_D and H_W curves

$$\left| \frac{\partial H_D}{\partial r} \right| > \left| \frac{\partial H_W}{\partial r} \right|. \tag{8}$$

In general, a bias field (H_{bias}) is needed to secure the intersection at "b" which satisfies (8). Refer to Fig. 15 and note that an $H_W + H_{bias}$ curve

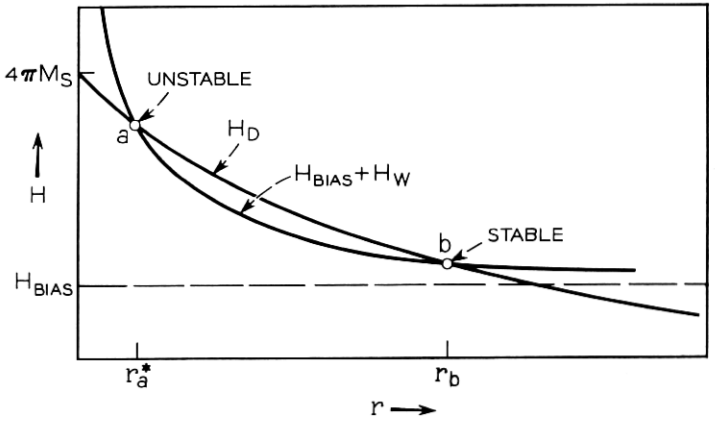

Fig. 15 — A stable cylindrical domain can be obtained if a suitable bias field is applied.

is plotted. For a radius somewhat greater than r_b the combined wall and applied fields close the domain to r_b. If the starting radius is less than r_b but greater than r_a^* the dominant magnetostatic field will open the domain to r_b. Any domain of radius less than r_a^* will collapse. By adjusting the bias field r_b can be varied somewhat. For example, in $TmFeO_3$, 2.3 mils thick, r_b can be varied from 2.8 mils to 1.2 mil as the bias field is changed from 26 Oe to 36 Oe.

As H_{bias} is increased, r_a^* and r_b approach each other and become equal when the $H_W + H_{bias}$ curve is tangential to the H_D curve. With a further increase, all cylindrical domains become unstable and collapse. This leads to a direct method of obtaining the wall energy density, σ_W.

IV. WALL ENERGY DENSITY, σ_W

The cylindrical domain radius r_b as a function of an applied field H_{bias} has been measured for a number of rare earth orthoferrites. A typical curve of domain radius vs applied field is plotted in Fig. 16. This experiment, as was pointed out above, is a direct method for obtaining σ_W the domain wall energy density.

For the 2.3-mil thick platelet of $TmFeO_3$ described previously the minimum r observed is 1.15 mil at an applied field of 36 Oe. Since $h = 2.3$ mils, $2r/h = 1$. From Fig. 24, $H_D/4\pi M_s = 0.58$. For $TmFeO_3$ $4\pi M_s = 140$ gauss so $H_D = 81$ Oe. Thus, $H_W = H_D - H_{bias} = 81 - 36 = 45$ Oe. Therefore,

$$\sigma_W = 2rH_WM_s$$
$$= 2.80 \text{ ergs/cm}^2.$$

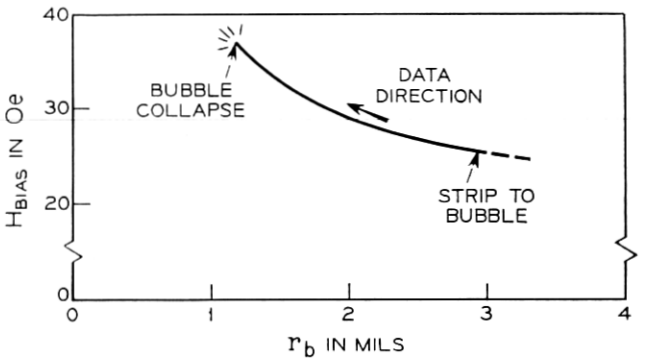

Fig. 16 — Cylindrical domain size as a function of an applied bias field.

The average results obtained on orthoferrites for which platelets were available are tabulated in Table I. Note that in addition to the measured values of $r_{\min}$ that a calculated $2\pi r_a$ (Section 3.31) is also included. Thiele[5] has shown that $2\pi r_a$ is the optimum platelet thickness. Platelets of thickness $2\pi r_a$ will sustain cylindrical domains of the minimum possible diameter and this diameter will be approximately $2\pi r_a$. Note that $TmFeO_3$ has the lowest calculated $2\pi r_a$ (as well as the lowest observed domain size), and is thus a prime contender for device applications. It is hoped that some other orthoferrite such as $YFeO_3$ which has a reported[7] σ_W of 1.0 erg/cm^2 and $4\pi M_s$ of 105 gauss may give yet smaller domains than $TmFeO_3$.

V. GENERAL COMMENTS AND OBSERVATIONS

The sequence of pictures of Fig. 17 give a pictorial display of much of the material described in the preceding sections. An "as grown" $TmFeO_3$ platelet, 2.3 mils thick was subjected first to an increasing bias field applied parallel to the c-axis (perpendicular to the planar face) and then to a decreasing field.

The platelet is demagnetized, i.e., equal areas of magnetization up and down, if no field is applied (a). The average width of a domain is the consequence of a magnetostatic and wall energy balance and as such can be used to obtain a crude estimate of the wall energy. It is an observation that for very thick or very thin samples the strip width is increased from that shown.

As the field is increased, the dark strips narrow and there is a general reshuffling of domains. At (g) one of the "dumbell" domains has collapsed into a cylindrical domain. Further increase in field finds a total of five such domains (i). At 37 Oe applied field, three of the five have collapsed (j) and the remaining two would also collapse if a few more tenths of an oersted was applied. However, at this point

TABLE I

			Observed			Calculated
Orthoferrite	$4\pi M_s$[6] (gauss)	σ_W (ergs/cm^2)	$2r_{\min}$ (mils)	Field (Oe)	Thickness (mils)	$2\pi r_a$ (mils)
$HoFeO_3$	91	2.0	4.6	12	2.1	3.8
$ErFeO_3$	81	1.7	6.0	8	2.0	4.1
$TmFeO_3$	140	2.8	2.4	36	2.3	2.2
$YbFeO_3$	143	3.0	3.8	59	4.4	2.3
$LuFeO_3$	119	3.9	8.8	4	1.4	4.3

the field was slowly reduced and the two cylindrical domains grew in size. At 27 Oe they became unstable as circles and blew out into strips (*k*). The circle to strip to circle process can be repeated with a field perturbation of 1.5 oersted. Thus, the wall coercivity, H_c, is probably less than $1.5/2 = 0.75$ oersted. If the field is reduced to zero a pattern superficially like (*a*) appears.

By passing the tip of a fine magnetized wire over the surface of a demagnetized platelet it is possible to "cut" through the strip domains. Then as the bias field is applied large numbers of "bubbles" appear such as in Fig. 18. Our next problem is to look at the ways in which these "bubbles" can be manipulated to do logic and storage.

It will suffice, for the purposes of this article, to just indicate very briefly some of the operations that are possible. These are illustrated in Fig. 19. Since in the correct environment cylindrical domains have been shown to be stable, *storage* is readily available. *Transmission* of a domain from location 1 to location 2 is achieved by energizing a conductive loop located at position 2. The domain, in seeking the lowest energy state, readily moves to position 2. To obtain a complete set of logic functions an *interaction* is required. The magnetostatic repulsion which exists between domains ensures that only one domain will move into position 2 if that loop is energized. New domains can be created by *replication*. This involves literally tearing a single domain into two halves which then expand to full size. The use of the full set of operations allows the possibility of data processing applications.

It is apparent that a multi-dimensional shift register can be built using *transmission* with a three-phase drive source to achieve the desired directionality. Information is inserted by selective *replication* at the input of the register. Most of the early device work has centered on the design and operation of multi-dimensional shift registers. Initial success was obtained when a 2.2-mil thick platelet of $HoFeO_3$ was combined with a waffle-iron like high-permeability ferrite baseplate[8] The baseplate consisted of a matrix of 10-mil by 10-mil posts positioned on 15-mil centers. Single turn windings were wrapped about selected posts and series connected to form the five distinct propagation phases identified in Fig. 20(f). The waffle-iron posts served to facilitate the wiring procedure as well as to precisely define the applied field patterns. Assume as shown in (a) that domains exist in the orthoferrite platelet at the upper left and middle left $\Phi 1$ locations. The location of the domains can be ascertained by viewing the results

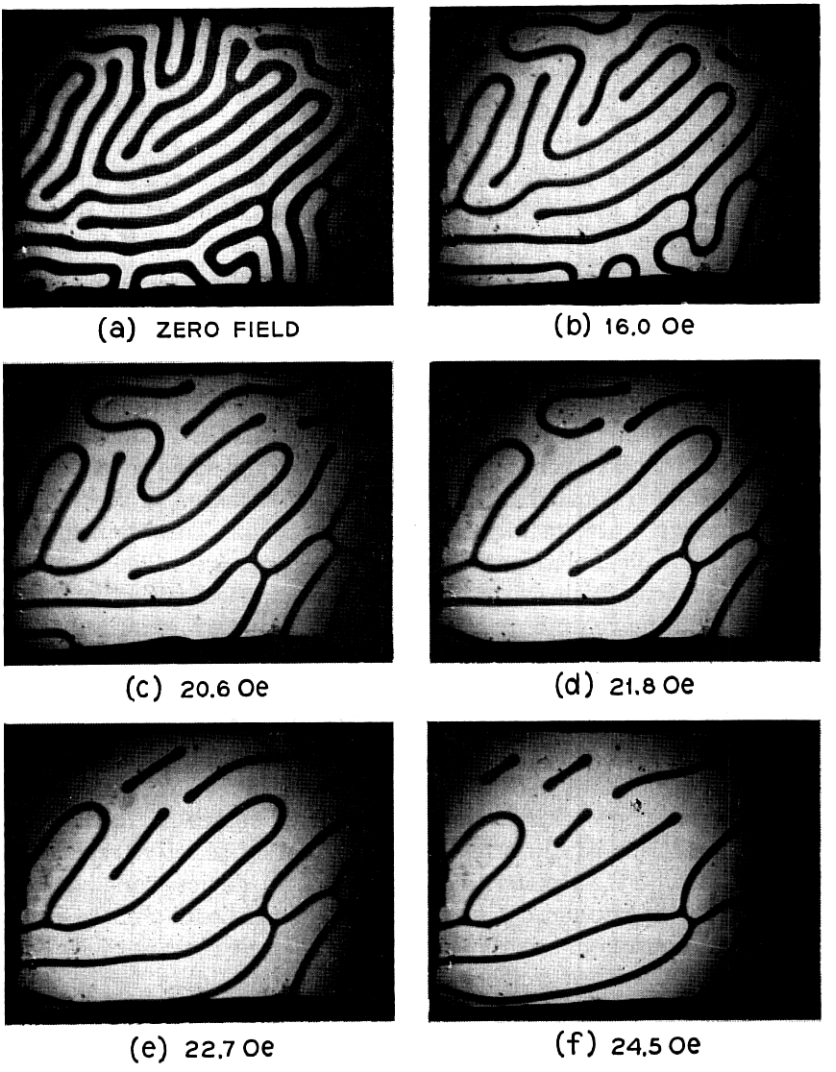

Fig. 17 — Faraday studies of a platelet $TmFeO_3$ orthoferrite, 2.3 mils thick, c-axis normal to the surface. Sample originally demagnetized (a). Field applied normal to the surface, first increased, then decreased. Note at (g) that the strip in the upper left-hand corner became a cylindrical domain. This, and the other

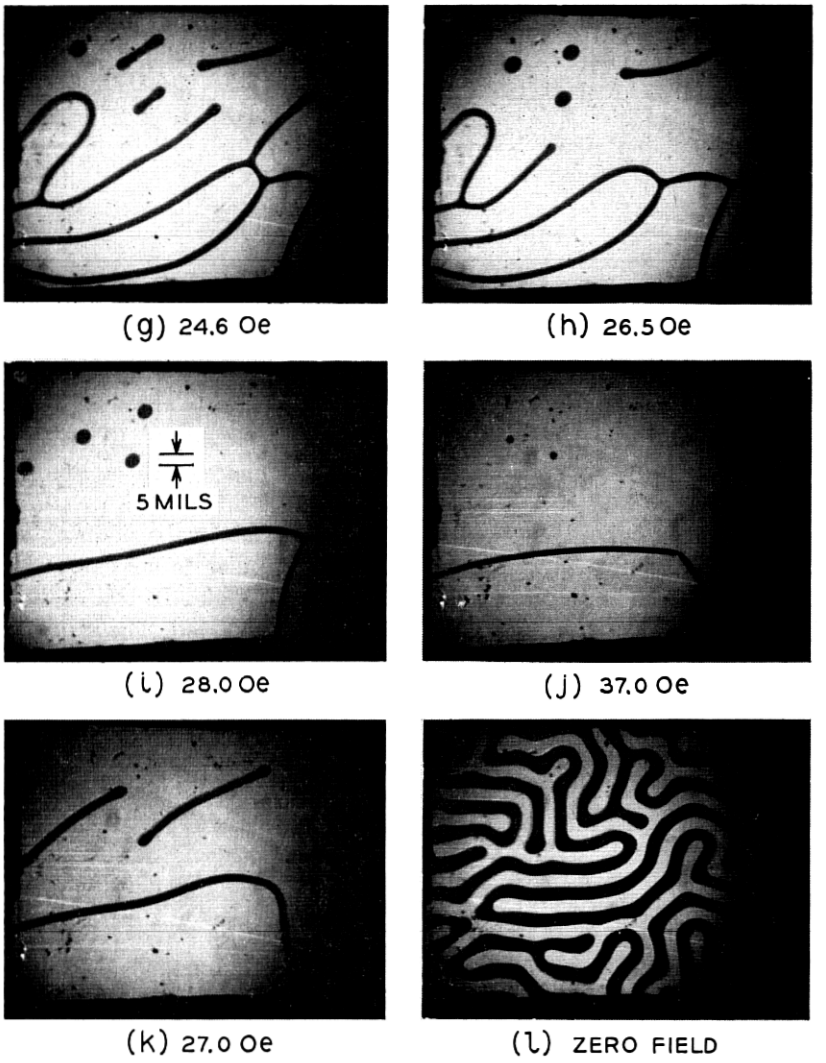

Fig. 17 — (continued)
cylindrical domains which formed, reduced in size until (j) when three of five collapsed. As the field is decreased the remaining two bubbles open into strips (k) and eventually grow to fill the entire platelet (1).

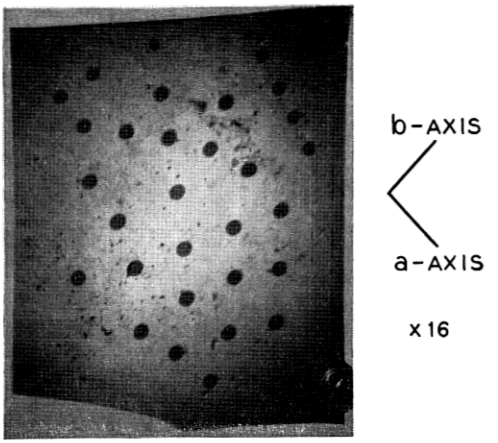

Fig. 18 — Numerous cylindrical domains produced by "cutting" strip domains with a magnetized wire.

of a magnetic colloid interaction with the domain walls defining the cylindrical domains. Application of a current pulse to Φ2 causes the pair of domains to step one post position to the right. In this manner the domain patterns of (b) through (d) are generated. The sequence 123145132154 . . . causes domains to propagate clockwise in the upper and lower loops resulting in a residual pattern (e) being generated by the colloid.

More recent work has been directed toward improving the storage density of the shift register. Operation with 3.5-mil diameter domains has been achieved and there is every indication that sub-mil domains can also be propagated. The final storage density of the device ap-

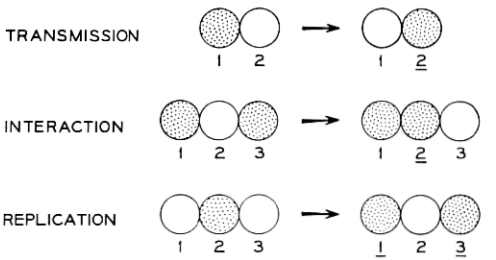

Fig. 19 — Illustration of transmission, interaction, and replication. Shaded areas represent cylindrical domains, circles the drive loops, and underlined numbers the energized loops.

pears to be limited by wiring pattern resolution rather than any magnetic property.

VI. CONCLUSIONS

A variety of experiments have been performed on orthoferrites. These include cylindrical domain stabilities, strip stabilities, magnetostatic interactions, and device applications. It has been found that the concept explained in the body of this memorandum of considering the magnetostatic and wall energies as generating equivalent fields, is useful toward a first order understanding of the phenomenon observed.

Cylindrical domain stability has been studied in detail. The wall energy density σ_W and the magnetic moment $4\pi M_s$ are seen to be significant factors limiting the minimum available diameter of a cylindrical domain. With experiments completed on five of fourteen orthoferrites the results have shown that $TmFeO_3$ has the smallest stable domain diameter, 2.3 mils. There is every reason to expect that submil domains will be realized in other orthoferrites.

This paper has discussed idealized, elastic, domains. However, most of the early successes in manipulating domains in shift register, logic, and memory structures were accomplished with rather thin, high coercivity platelets. Further study will be required to determine the optimum blend of operating characteristics.

VII. ACKNOWLEDGMENTS

Many people have contributed directly to the orthoferrite studies. Samples were furnished by J. P. Remeika, L. G. Van Uitert, and W. H. Grodkiewicz, with inspiration by H. E. D. Scovil, W. Shockley, and U. F. Gianola. Special thanks must be given to R. C. Sherwood for initially suggesting the orthoferrites and A. Thiele for his derivations and many helpful discussions.

APPENDIX A

It is desired to derive the average z-component field $\bar{H}_z$ acting on the domain walls which define a strip of magnetization reversal of width W located in an infinitely large magnetic platelet of thickness h. See Fig. 21. Consider the domain wall located in the $X = 0$ plane. Note that the surface magnetic charge of the strip itself and that of an image strip also of width W will produce cancelling fields at any

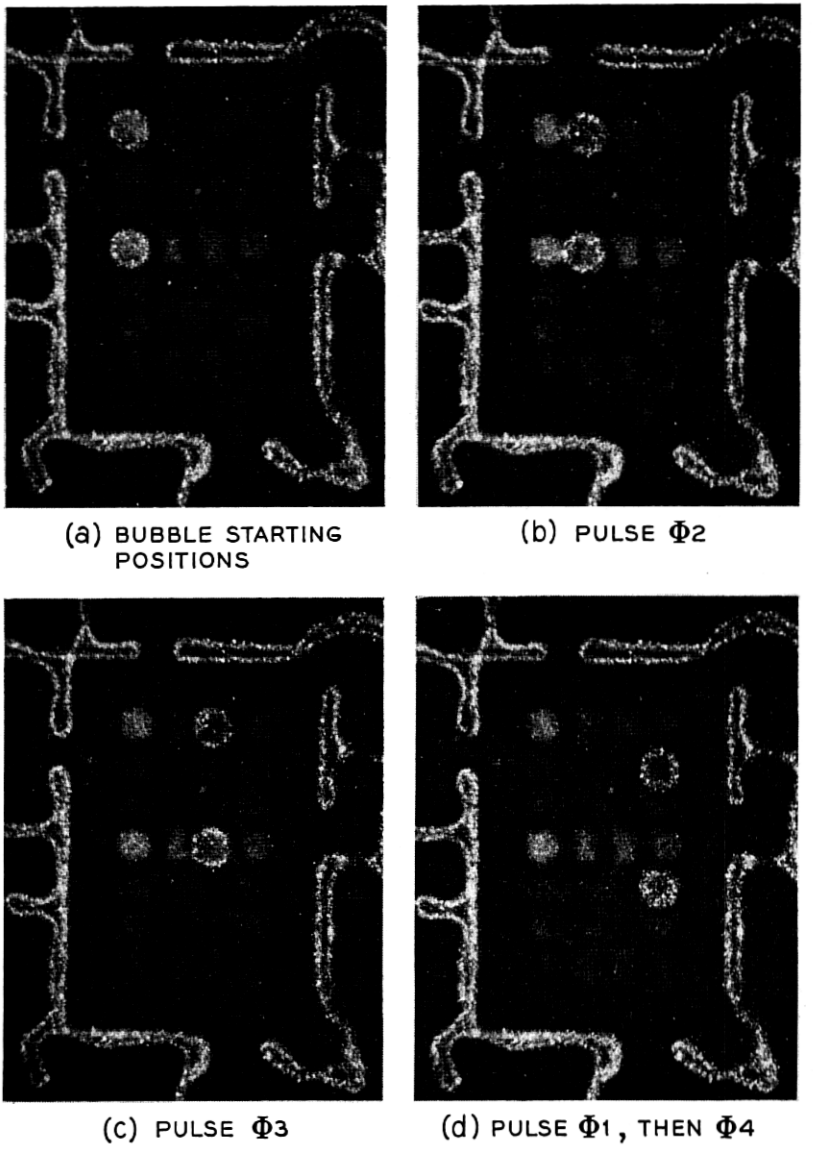

Fig. 20 — Sequence of photographs illustrating two-dimensional shifting of cylindrical magnetic domains in $HoFeO_3$ orthoferrite. Operation was obtained on a ferrite waffle-iron baseplate and observed with a 3M Colloid Viewer.

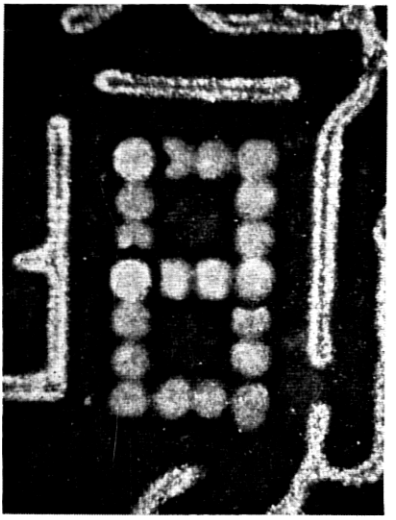

(e) RESIDUAL PATTERN IN COLLOID VIEWER AFTER CONTINUOUS 123145132154 SEQUENCE

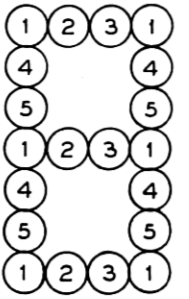

(f) IDENTIFICATION OF DRIVE LOOP DESIGNATIONS

Fig. 20 — (continued)

"z" and thus need not be considered. The field at "z" due to the upper right-hand sheet of charge is

$$\frac{H_z}{4\pi M_s} = \frac{1}{2\pi} \tan^{-1}\left(\frac{z}{W}\right).$$

Now

$$\bar{H}_z = \frac{1}{h}\int_0^h H_z\, dz.$$

This equation assumes that the domain wall is rigid and therefore that the force acting on the wall can be averaged.
So

$$\frac{\bar{H}_z}{4\pi M_s} = \frac{1}{2\pi h}\int_0^h \tan^{-1}\left(\frac{z}{W}\right) dz$$

$$= \frac{1}{2\pi}\left[\tan^{-1}\left(\frac{h}{W}\right) - \frac{W}{2h}\ln\left(1 + \frac{h^2}{W^2}\right)\right].$$

Since four sheets of magnetic charge are acting on the wall (producing components identical in field direction and magnitude) the total

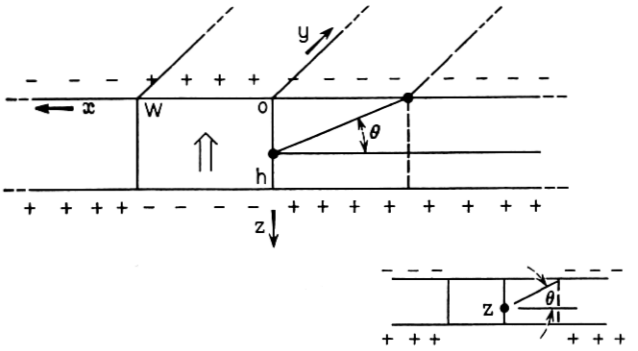

Fig. 21 — Identification of parameters used in the derivation of the strip magnetostatic field.

average field becomes

$$\frac{\bar{H}_z}{4\pi M_s} = \frac{2}{\pi}\left[\tan^{-1}\left(\frac{h}{W}\right) - \frac{W}{2h}\ln\left(1 + \frac{h^2}{W^2}\right)\right].$$

In the body of the text (Section 3.1) the z-component of field for the strip is designated H_s and the above expression is entered as (2).

The assumption that the walls defining the strip domain are rigid (and straight) is a good approximation for $W \gg h$ and poor for $W \ll h$. In the latter case, the average force acting on the walls differs significantly from the maximum forces experienced by the walls. It is expected that for $W \ll h$ the walls will bulge outward.

APPENDIX B

The calculation of the average wall field $\bar{H}_z$ produced by surface magnetic charge, for a circular magnetic domain proceeds in much the same manner as for the strip. As in the strip case the domain wall itself is assumed to be rigid. The mathematics are simplified if it is recognized that a cancellation cylinder exists as shown in Fig. 22. Only one quadrant will be considered with a factor of eight included to account for all four quadrants plus a top and bottom.

In general, as defined in Fig. 23,

$$H_z = \int \frac{M_s \cos\alpha \, dA}{r^2}$$

so

$$\frac{H_z}{8M_s} = \int_0^{\pi/2}\int_{2r_0 \sin\theta}^{\infty} \frac{\rho z \, d\rho \, d\theta}{(\rho^2 + z^2)^{\frac{3}{2}}}.$$

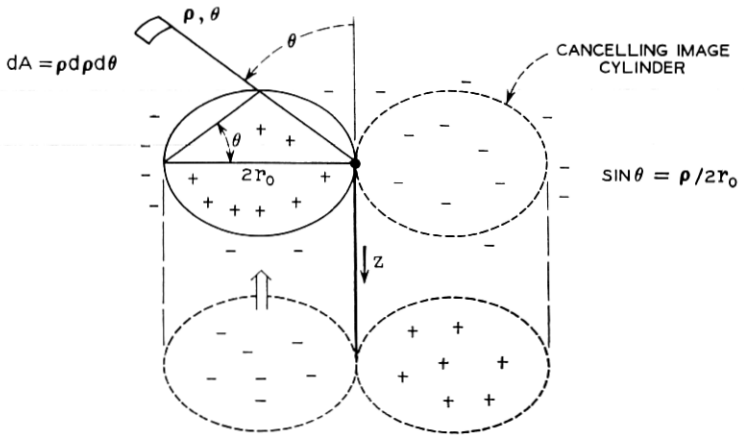

Fig. 22 — Figure useful in the derivation of the average wall field of a cylindrical domain produced by surface magnetic charge.

Using

$$\bar{H}_z = \frac{1}{h}\int H_z\, dz$$

$$\frac{\bar{H}_z h}{8M_s} = \int_0^{\pi/2}\int_{2r_0\sin\theta}^{\infty}\int_0^h \frac{z\, dz\, \rho\, d\rho\, d\theta}{(\rho^2+z^2)^{\frac{3}{2}}}$$

$$= -\int_0^{\pi/2}\int_{2r_0\sin\theta}^{\infty} \frac{\rho\, d\rho\, d\theta}{(\rho^2+z^2)^{\frac{1}{2}}}\Bigg|_0^h$$

$$= \int_0^{\pi/2}\int_{2r_0\sin\theta}^{\infty}\left[1 - \frac{\rho}{(\rho^2+h^2)^{\frac{1}{2}}}\right] d\rho\, d\theta$$

$$= \int_0^{\pi/2}\left[\rho - (\rho^2+h^2)^{\frac{1}{2}}\right] d\theta\Bigg|_{2r_0\sin\theta}^{\infty}$$

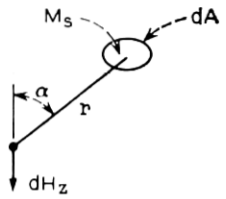

Fig. 23 — Figure showing field H_z is related to M_s and the angle α.

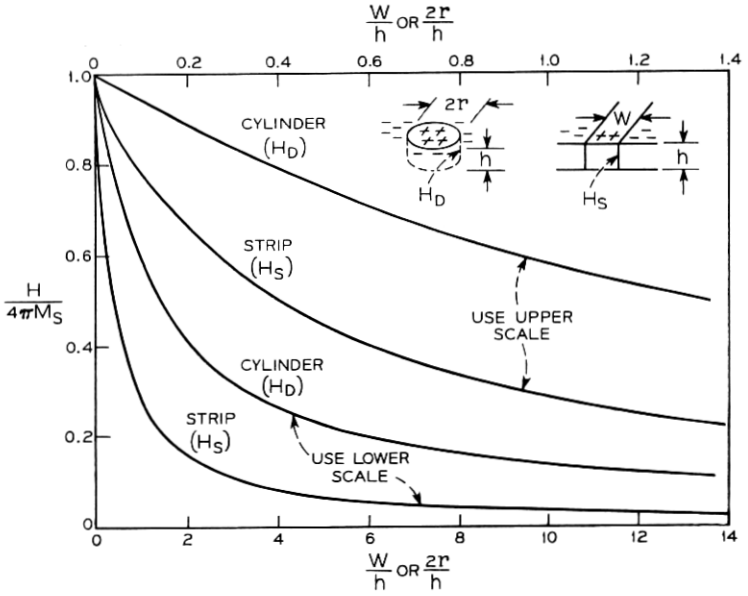

Fig. 24 — Cylinder and strip magnetostatic fields.

$$= \int_0^{\pi/2} (4r_0^2 \sin^2\theta + h^2)^{\frac{1}{2}}\, d\theta - \int_0^{\pi/2} 2r_0 \sin\theta\, d\theta$$

$$= h \int_0^{\pi/2} \left(1 + \frac{4r_0^2}{h^2}\sin^2\theta\right)^{\frac{1}{2}} d\theta - 2r_0 .$$

Letting $\sin^2\theta = 1 - \cos^2\theta$,

$$\frac{\bar{H}_z h}{8M_s} = h\sqrt{1 + \frac{4r_0^2}{h^2}} \int_0^{\pi/2} \left[1 - \frac{4r_0^2/h^2}{1 + \frac{4r_0^2}{h^2}} \cos^2\theta\right]^{\frac{1}{2}} d\theta.$$

But

$$\int_0^{\pi/2} (1 - k^2\cos^2\theta)^{\frac{1}{2}}\, d\theta = \int_0^{\pi/2} (1 - k^2\sin^2\theta)^{\frac{1}{2}}\, d\theta.$$

So the final result can now be written as

$$\frac{\bar{H}_z}{4\pi M_s} = -\frac{4r_0}{\pi h} + \frac{2}{\pi}\sqrt{1 + \frac{4r_0^2}{h^2}} \int_0^{\pi/2} \left[1 - \left(\frac{1}{1 + \frac{h^2}{4r_0^2}}\right)\sin^2\theta\right]^{\frac{1}{2}} d\theta.$$

The integral is the complete elliptic integral of the second kind $E(k, \pi/2)$ where

$$k^2 = \frac{1}{1 + \frac{h^2}{4r_0^2}}.$$

In the text, the magnetostatic field effective on the cylindrical domain wall is designated H_D thus the final expression, which is (5), becomes

$$\frac{H_D}{4\pi M_s} = \frac{2}{\pi}\left[-\frac{2r_0}{h} + \sqrt{1 + \frac{4r_0^2}{h^2}}\, E(k, \pi/2)\right].$$

Equation (5) and (2), representing the magnetostatic field of the cylinder and strip, respectively, are plotted in detail in Fig. 24.

REFERENCES

1. Michaelis, P. C., A New Method of Propagating Domains in Thin Ferromagnetic Films, International Congress on Magnetism, 1967.
2. Spain, R. J., et al., J. Appl. Phys., 1965, p. 1103.
3. Sherwood, R. C., Remeika, J. P., and Williams, H. J., Domain Behavior in Some Transparent Magnetic Oxides, J. Appl. Phys., *30,* February 1959, pp. 217–225.
4. Kooy, C. and Enz, U., Experimental and Theoretical Study of the Domain Configuration in Thin Layers of $BaFe_{12}O_{19}$, Philips Research Report, *15,* Feb. 1960, pp. 7–29.
5. Thiele, A., private communication.
6. Sherwood, R. C. and Van Uitert, L. G., private communication.
7. Umebayashi, H. and Ishikawa, Y., Motion of a Single Domain Wall in a Parasitic Ferromagnet $YFeO_3$, JPS of Japan, *20,* December, 1965.
8. Bobeck, A. H., The Cubic Waffle-Iron Memory, 1963 Proc. Intermag. Conference, April, 1963.